Cruz Biotechnology. Anti-TPX2 antibody was purchased from Novus Biologicals.

Formalin-fixed and paraffin-embedded liver tissues containing HCC were obtained from the National Cancer Center Hospital, and stained as described previously (15, 16). Immunoblot analysis of the KIM-1 cell lysate was done as described previously (15).

Animal experiments. Eight million KIM-1 cells suspended in 0.1 mL of PBS were s.c. inoculated into the flanks of 5-week-old female BALB/c nu/nu nude mice (SLC). Eight days later, the tumor-bearing mice were treated with siRNA together with atelocollagen (Koken Co., Ltd.), as described previously (17, 18). The final concentration of siRNA and atelocollagen was 11 μmol/L and 0.5%, respectively, and 200 μL of the siRNA solution were injected directly into each tumor. Tumor volume was determined every 3 days using the formula $V = 1/2\ (A \times B^2)$, where A and B represent the largest and smallest dimensions of the tumor, respectively.

Animal experiments were reviewed by the institutional ethics committee and performed in compliance with the

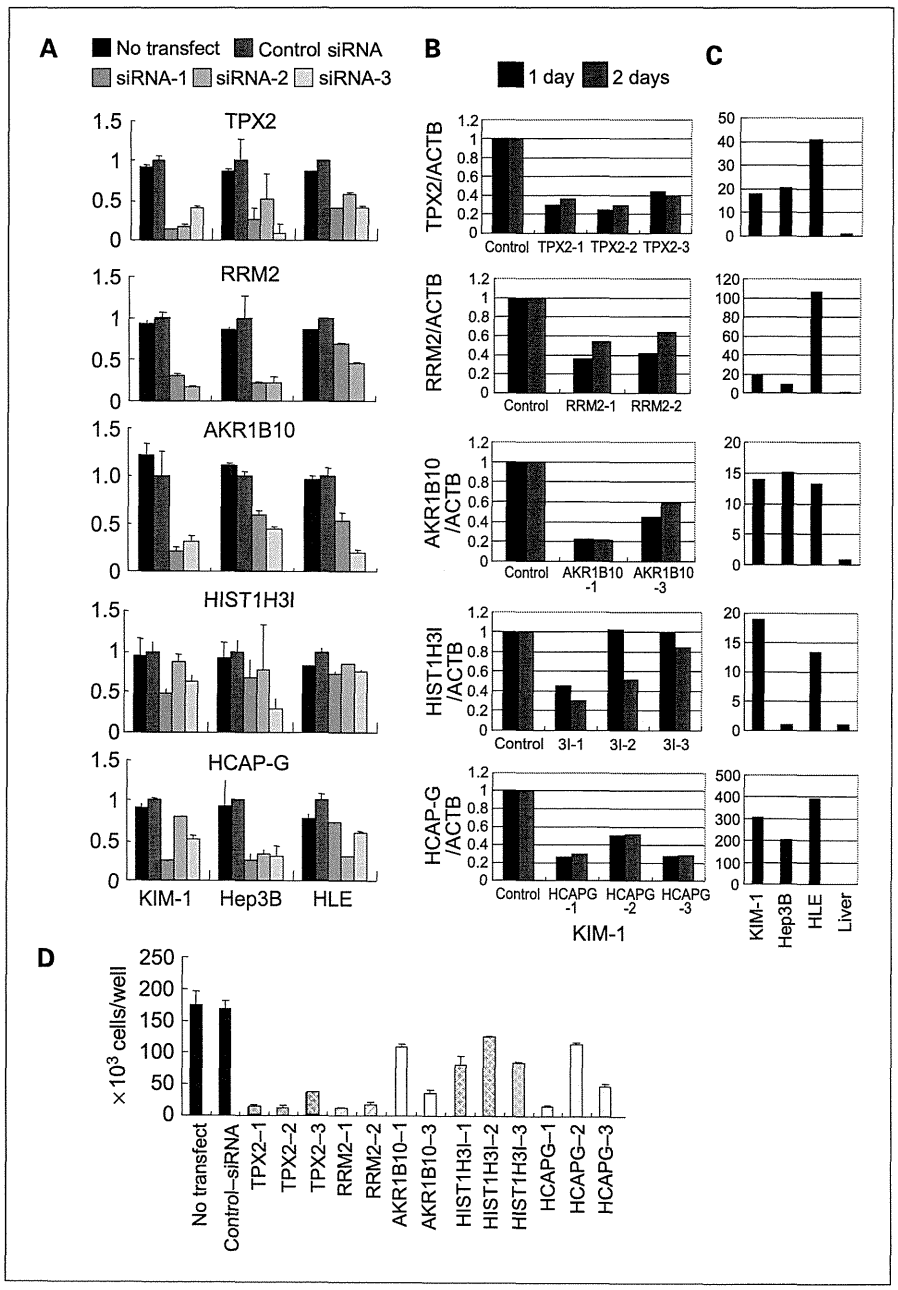

Fig. 2. siRNA-based functional screening. A, siRNA-mediated screening of genes required for proliferation of HCC cells. Three HCC cell lines (KIM-1, Hep3B, and HLE) were transfected with the indicated siRNAs, and the relative proportion of living cells was assessed 3 days later by measuring the mitochondrial succinate-tetrazolium reductase activity. Values for control siRNA were set at 1. B, reduction of the level of mRNA for each gene was determined by real-time PCR 1 and 2 days after transfection of KIM-1 cells with the indicated siRNAs. Values for control siRNA were set at 1. C, expression of each gene in HCC cell lines (KIM-1, Hep3B, and HLE) and normal liver tissue. D, confirmation of siRNA-mediated inhibition of HCC cell proliferation. KIM-1 cells were transfected with the indicated siRNAs, and the number of living cells was counted 3 days later by trypan blue dye exclusion using a hemocytometer.

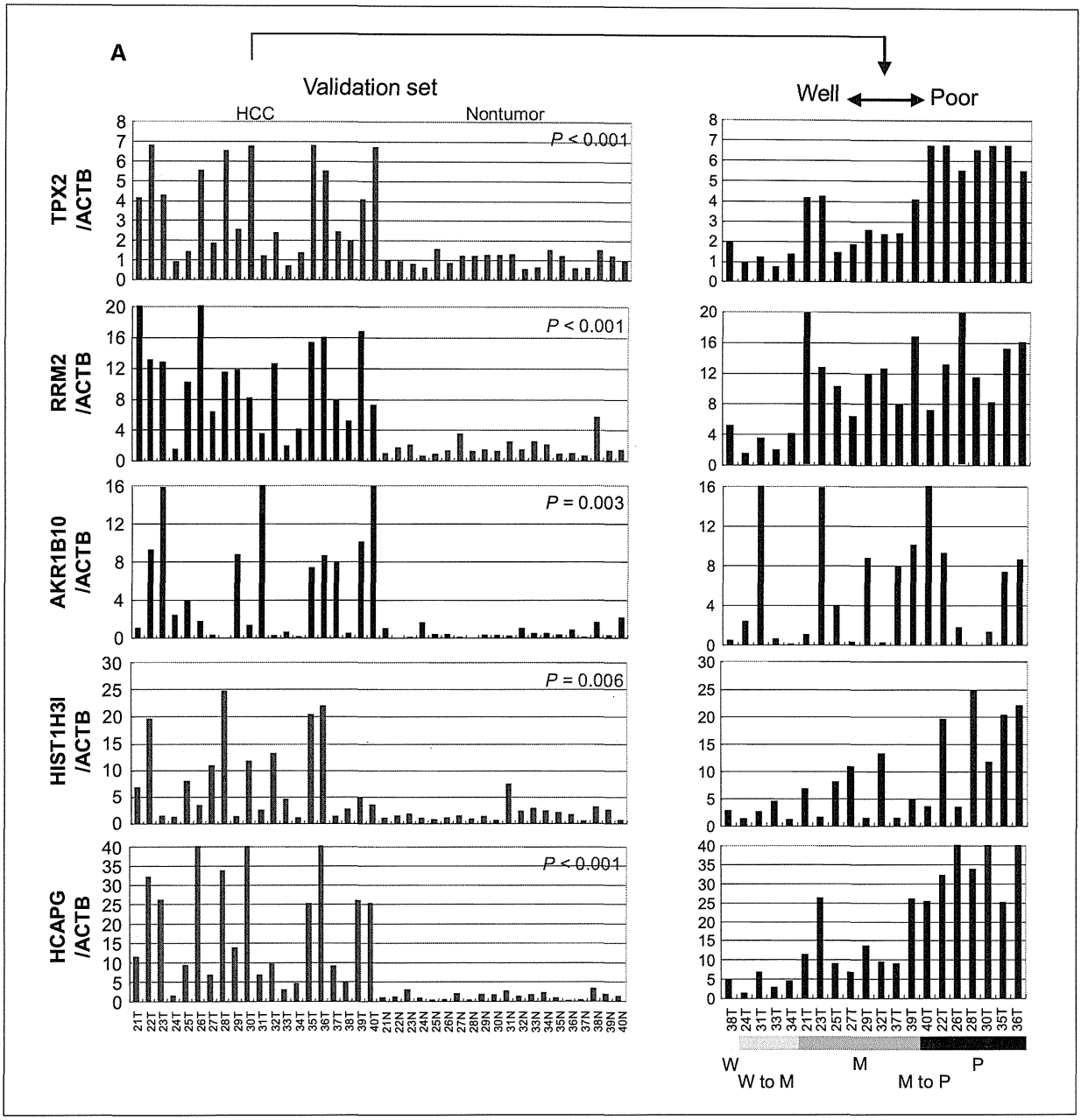

Fig. 3. Validation of differential expression. A, mRNA expression levels of selected genes in 20 independent pairs of HCC (21-40T) and adjacent nontumorous liver tissue (21-40N; validation set 1) determined by real-time PCR (left). The expression levels in HCC were realigned according to histologic differentiation (right). W, well differentiated; W to M, well to moderately differentiated; M, moderately differentiated; M to P, moderately to poorly differentiated, P, poorly differentiated.

guidelines for Laboratory Animal Research of the National Cancer Center Research Institute (Tokyo, Japan).

Statistical analysis. To extract differentially expressed genes from the array data, a paired *t* test with no correction was done (19) with asymptotic distribution to determine the *P* value. Correlations between array data and real-time PCR measurements were assessed using the Pearson correlation coefficient. The significance of differential gene expression between HCC and adjacent nontumorous liver tissue was assessed using the permutation paired *t* test followed by Bonferroni correction.

The weights and volumes of tumors are given as means (+SE). To evaluate the chronological effect of siRNAs on the growth of xenografts in comparison with control siRNA,

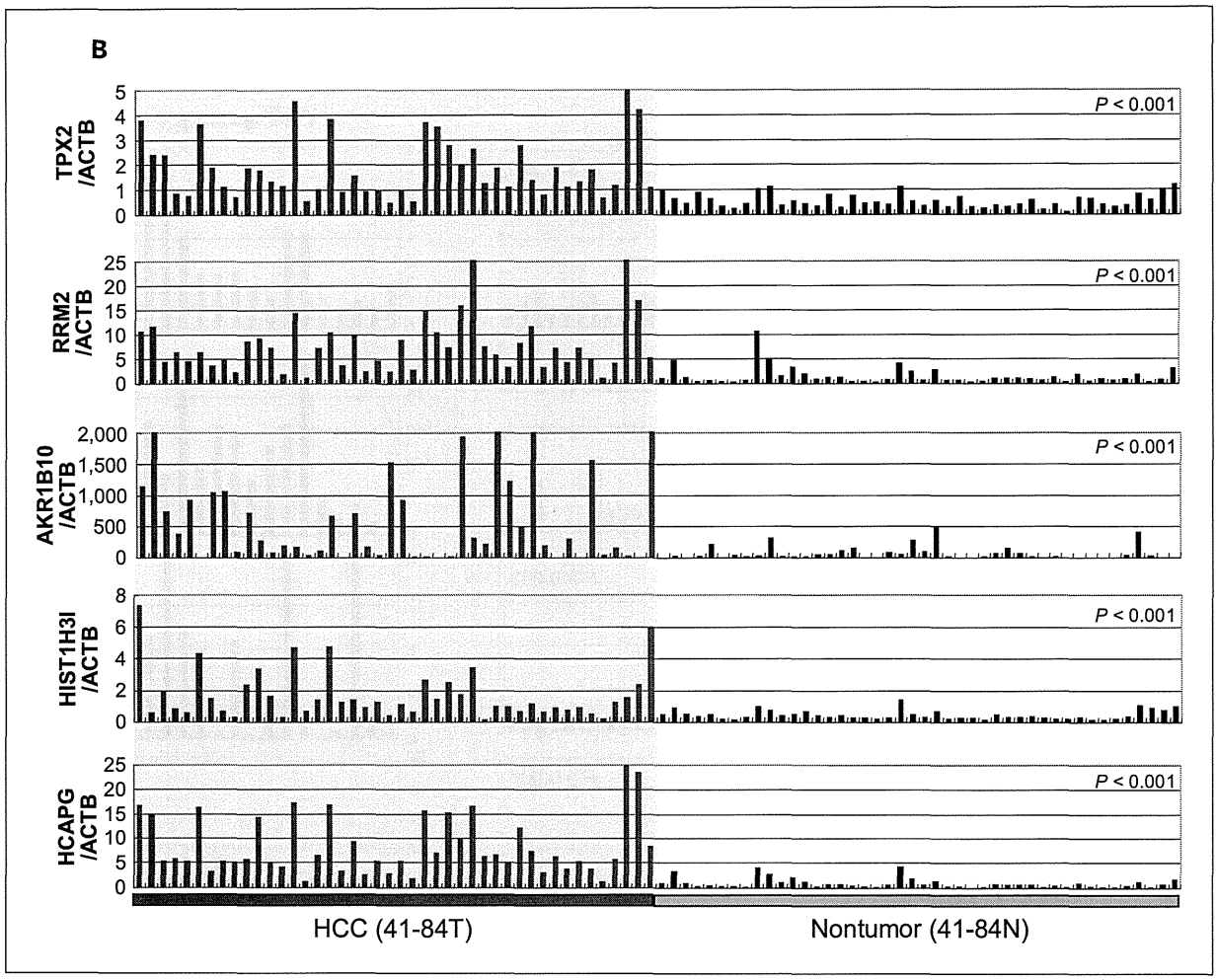

Fig. 3. *Continued.* B, expression levels of mRNAs for selected genes in 44 independent pairs of HCC (41-84T) and adjacent nontumorous liver tissue (41-84N; validation set 2) determined by real-time PCR.

a generalized linear mixed-effects model was used (20). The volume of the xenograft was modeled using γ-error distribution and log link function. This model considers each siRNA treatment as a fixed effect with control siRNA as an intercept and the number of days after implantation as a random effect. Estimates of variance components were obtained using the Laplacian approximation method, and the model fit was assessed using deviances. The significance of effects was estimated from the degree of freedom and t statistics followed by Bonferroni correction. Analysis was done using the lmer function for fitting generalized linear mixed-effects models, in the R statistical software package (version 2.6.0).

Results

Exon-based array analysis of HCC. Twenty paired samples of HCC and adjacent nontumorous liver tissue were subjected to genome-wide expression analysis using two different batches of the GeneChip Human Exon 1.0 ST arrays [discovery sets 1 (10 pairs) and 2 (10 pairs)]. Statistical analysis was done separately, and genes expressed differentially in the two sets were selected to eliminate any experimental bias caused by batch-to-batch variations. The exon array can detect mRNAs with low abundance as well as alternatively polyadenylated and spliced mRNA because the probes are designed to hybridize with the entire sequences of the transcripts (21). We identified 124 annotated genes that were differentially expressed between the background (nontumorous) liver tissue and HCC [at least a 3-fold change in transcription signal; $P < 0.001$ (paired t test with no correction)] in discovery set 1 (Supplementary Tables S2 and S3). The genes were clustered according to the similarity of their expression profiles (Fig. 1A), and the differential expression of representative genes was confirmed by real-time PCR (Fig. 1B). It was noteworthy that although 103 genes were found to be significantly downregulated, only 21 were apparently upregulated.

We selected 9 genes (*AKR1B10*, *ANLN*, *CCNB1*, *HIST1H3B*, *HIST1H3C*, *HIST1H3I*, *RRM2*, *TOP2A*, and *TPX2*) whose expression was upregulated in HCC (≥3-fold change in transcription signal; $P < 0.001$, *t* test) in both discovery sets 1 and 2. Furthermore, two additional genes (*HCAP-G* and *DEPDC1*) were selected using a different criterion (>2.5-fold change across all of the 20 cases in discovery sets 1 and 2, and a raw signal of <50 in all 20 of the nontumorous liver tissues; $P < 0.05$, *t* test).

RNAi-based screening of genes required for HCC cell proliferation. To identify genes that are essential for HCC cell proliferation, siRNA-based screening was done for the 11 genes that were upregulated in HCC. Two or three constructs of siRNA were designed for each gene. Relative cell viability was evaluated by the mitochondrial succinate-tetrazolium reductase activity-based assay 3 days after transfection (Fig. 2A). We selected five genes (*TPX2*, *RRM2*, *HCAP-G*, *HIST1H3I*, and *AKR1B10*) based on the criterion that at least two siRNAs per gene reproducibly suppressed cell proliferation by >20% in all of three cell lines (KIM-1, Hep3B, and HLE). Representative data are shown in Fig. 2A and B. The baseline expression of these genes was determined in the three cell lines by real-time reverse transcription-PCR (RT-PCR; Fig. 2C). We confirmed the cell proliferation–inhibitory activity of the siRNA by counting the numbers of cells (Fig. 2D).

Validation of differential gene expression in additional cases of HCC. The increased expression of the five genes selected using the siRNA-based screen was validated in 20 cases of HCC (validation set 1) by real-time PCR (Fig. 3A). The expression of all five genes was confirmed to be increased in HCC. The expression of *TPX2*, *RRM2*, *HCAP-G*, and *HIST1H3* was associated with loss of histologic differentiation (Fig. 3A, right). The expression of *AKR1B10* was upregulated in HCC regardless of differentiation. We further confirmed the differential expression of these genes between HCC and nontumorous liver tissues in 44 additional independent cases of HCC (validation set 2) by real-time PCR (Fig. 3B).

In the 18 normal organs examined, no significant expression of *TPX2*, *RRM2*, or *HCAP-G* was observed, except for the thymus (Fig. 4, left), which is largely involuted in nonjuvenile adults. No organs showed higher expression of *AKR1B10* than was the case in HCC. We did not select *HIST1H3I*, as this gene showed high expression in several vital organs (Fig. 4).

Protein expression analysis. Expression of the products of four candidate genes, *TPX2*, *HCAP-G*, *RRM2*, and *AKR1B10*, was examined immunohistochemically in 19 independent cases of HCC (Fig. 5). In 84% (16 of 19) of the cases, AKR1B10 protein was detected in the cancer but was hardly evident in the adjacent nontumorous liver tissue. The nuclear staining of HCAP-G and TPX2 was stronger in HCC than in the adjacent nontumorous liver in 42% (8 of 19) and 58% (11 of 19) of cases, respectively. Patchy staining of RRM2 was observed in 84% (16 of 19) of the HCCs.

***Inhibition of tumor growth* in vivo.** Finally, we performed an *in vivo* experiment to evaluate the feasibility of the four selected genes as therapeutic targets. siRNA against *AKR1B10*, *HCAP-G*, *RRM2*, and *TPX2* mixed with atelocollagen was injected into tumors (31.5 ± 1.9 mm^3) established by xenografting KIM-1 cells into the flank of nude mice (Fig. 6). Atelocollagen forms a complex with siRNA, thus enhancing its stability and allowing sustained release of siRNA *in vivo* (17, 18). The silencing of the target genes by each relevant siRNA was confirmed by real-time PCR (Fig. 6A). Treatments with siRNA against *AKR1B10*, *HCAP-G*, *RRM2*, or *TPX2* given twice, 1 week apart, significantly suppressed tumor growth (Fig. 6B; Supplementary Table S6), and the growth-inhibitory effects of siRNA were confirmed by weighing the excised tumors (Fig. 6C).

Discussion

There is now strong epidemiologic evidence that persistent infection with hepatitis B or C virus is a major cause of HCC. However, the precise molecular mechanism behind the development of HCC is still unclear. Mutation in the tumor suppressor gene *TP53* is most frequently observed in HCC associated with aflatoxin B exposure as well as chronic infection with hepatitis B and C viruses (22–24); however, it seems to be a late event during multistep carcinogenesis (22). Deregulation of the Wnt as well as other signaling pathways has been reported in HCC (22, 25). Therefore, a therapeutic method that can normalize these aberrantly activated oncogenic signals would be clinically valuable. In an attempt to discover therapeutic targets with high specificity for HCC, we searched for genes that are specifically upregulated in HCC in comparison with nontumorous liver tissue and normal vital organs using high-density microarrays designed to detect all the exons in the human genome (Figs. 1 and 4). This was followed by siRNA-based screening of genes required for HCC cell proliferation (Fig. 2) as well as quantitative RT-PCR analysis and immunohistochemistry of additional cases (Figs. 3 and 5). We finally identified four candidate genes and confirmed their functional involvement in the tumor growth of HCC xenografts (Fig. 6). These genes, *AKR1B10*, *HCAP-G*, *RRM2*, and *TPX2*, were expressed strongly and specifically in HCC, which is highly dependent on these genes for proliferation, and their feasibility as therapy targets also seems to be supported by the literature.

RRM2 is a subunit of ribonucleotide reductase that catalyzes the conversion of ribonucleoside 5′-diphosphates into their corresponding 2′-deoxyribonucleotides. Because this reaction is the rate-limiting step of DNA synthesis, and inhibition of ribonucleotide reductase stops DNA synthesis and cell proliferation, RRM2 has been considered a promising target for cancer therapy (26).

TPX2 (C20ORF1) is a microtubule-associated protein whose expression is restricted to the S, G_2, and M phases of the cell cycle. Suppression of TPX2 expression by RNAi causes defects in microtubule organization during mitosis,

leading to the formation of two microtubule asters that do not form a spindle (27). TPX2 is necessary for maintaining aurora A kinase in an active conformation (28, 29). Aurora kinases are essential for the regulation of chromosome segregation and cytokinesis during mitosis and have been reported to be overexpressed in a wide range of human tumors. Several aurora kinase inhibitors, such as VX-680/MK-0457, have been showed to have anticancer effects *in vitro* and *in vivo* (30, 31). The binding of TPX2 modulates the conformation of aurora A and reduces its affinity

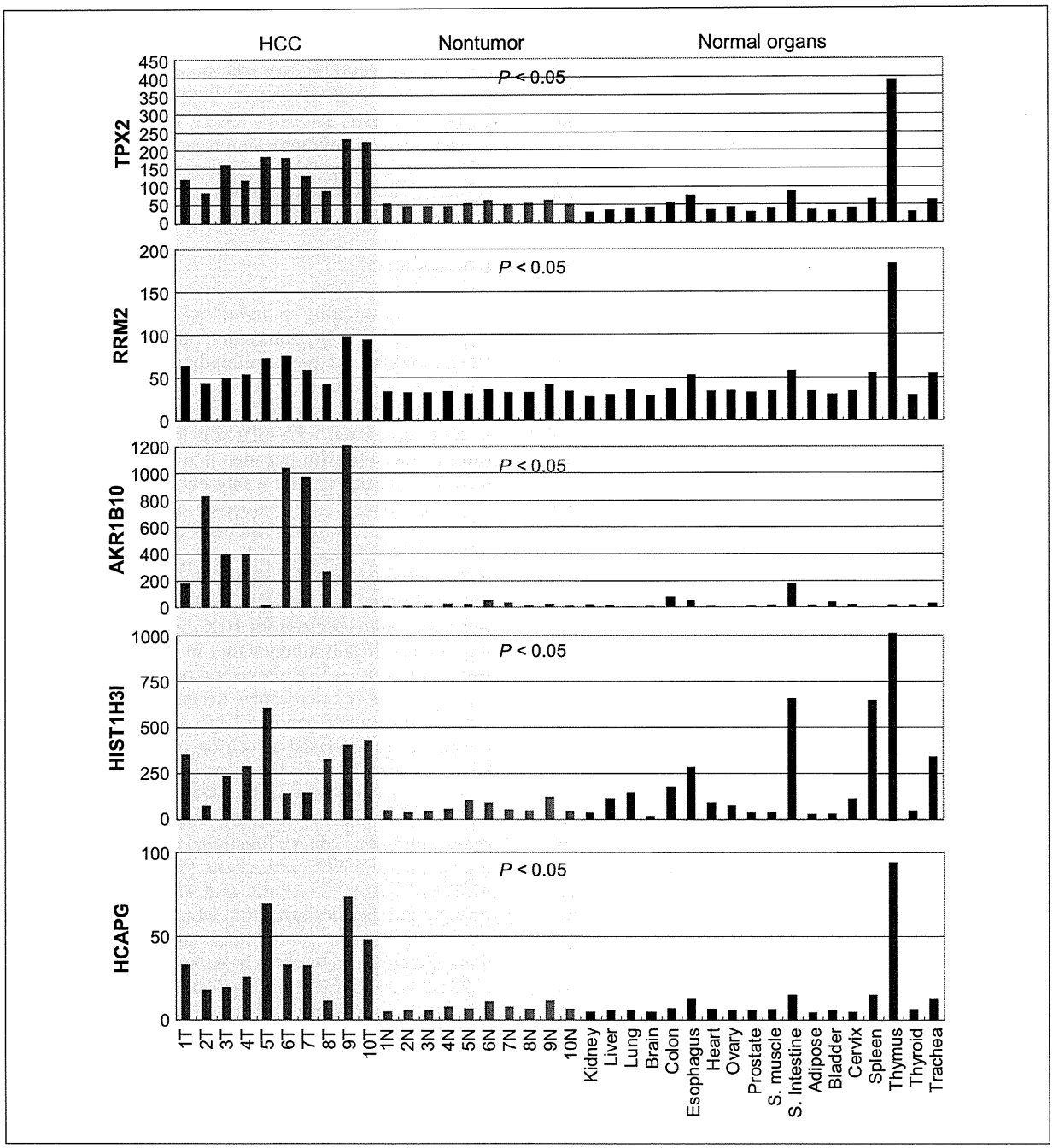

Fig. 4. Expression in normal organs. Expression levels of mRNAs for selected genes in 10 pairs of HCC (1-10T) and adjacent nontumorous liver tissue (1-10N; discovery set 1) and 18 normal organs determined by Human Exon 1.0 ST arrays (shown in arbitrary units). The significance of differential expression between HCC and adjacent nontumorous liver tissue was assessed using permutation paired *t* test, and Bonferroni-corrected *P* values are provided. S. muscle, skeletal muscle; S. intestine, small intestine.

for VX-680 (32). Inhibition of TPX2 may increase the efficacy of this class of aurora kinase inhibitors.

HCAP-G is a component of the condensin complex that organizes the coiling topology of individual chromatids. Condensin also contributes to mitosis-specific chromosome compaction and is required for proper chromosome segregation, although the functional significance of HCAP-G in the condensing complex is largely unknown (33, 34).

AKR1B10 (ARL1, aldose reductase-like 1) was originally isolated as a new member of the aldo-keto reductase superfamily overexpressed in HCC and is reportedly related to the histologic differentiation of HCC (35, 36). AKR1B10 was also overexpressed in squamous cell carcinoma of the lung and its precursor conditions (37). Because the expression of AKR1B10 was highly specific to HCC and its inhibition suppressed tumor growth (Fig. 6), chemicals that specifically inhibit AKR1B10 activity may be useful anticancer drugs with minimal side effects.

It cannot be denied that many important genes were probably overlooked at every step of the present screen,

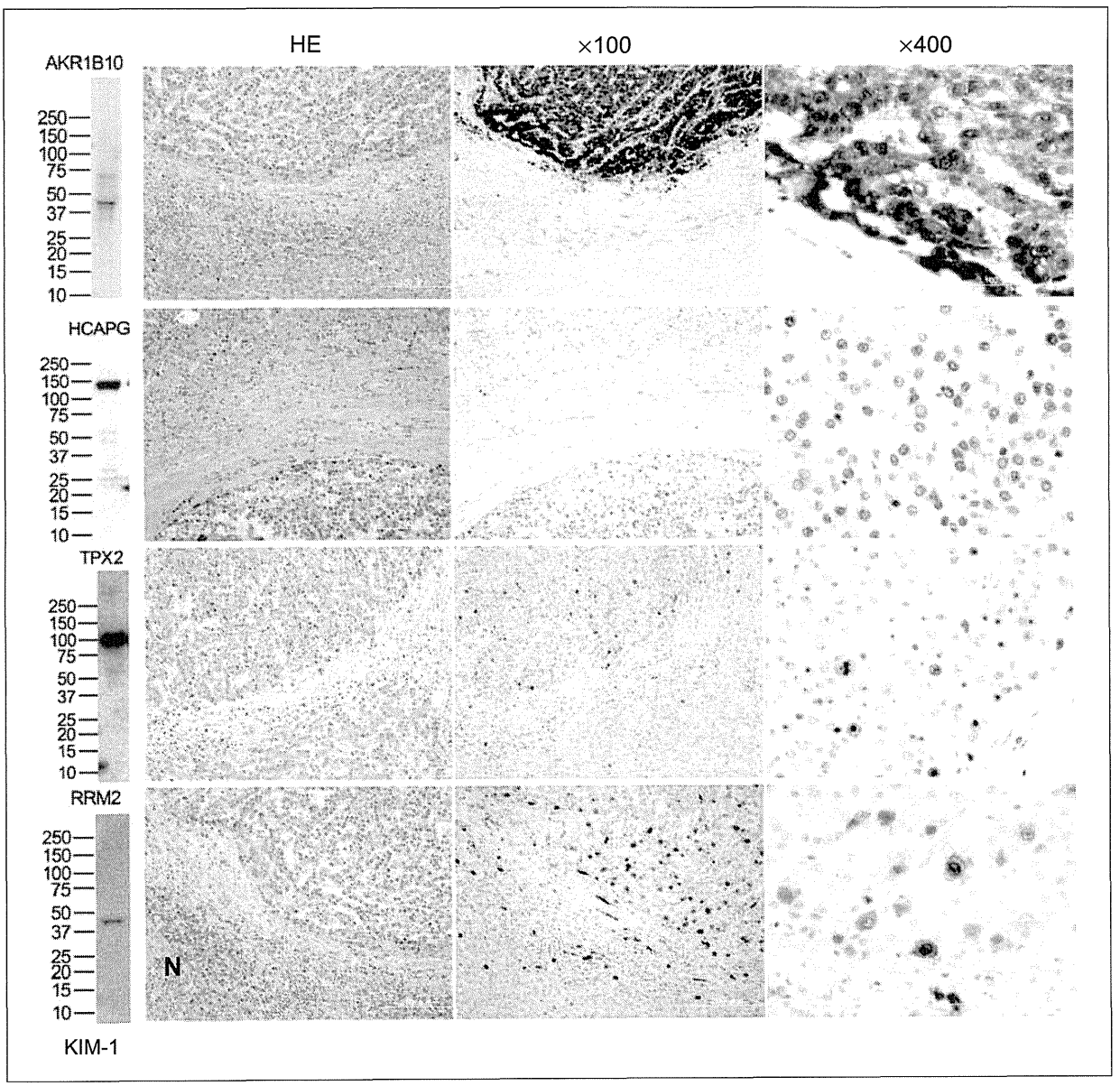

Fig. 5. Protein expression in HCC. Hematoxylin and eosin (HE) staining (original magnification, × 100) and immunoperoxidase staining (original magnifications, × 100 and × 400) of AKR1B10, HCAP-G, RRM2, and TPX2 proteins in HCC and adjacent nontumorous liver tissue. The specificity of antibodies was determined by immunoblotting of the KIM-1 cell lysate (left). N, nontumorous liver.

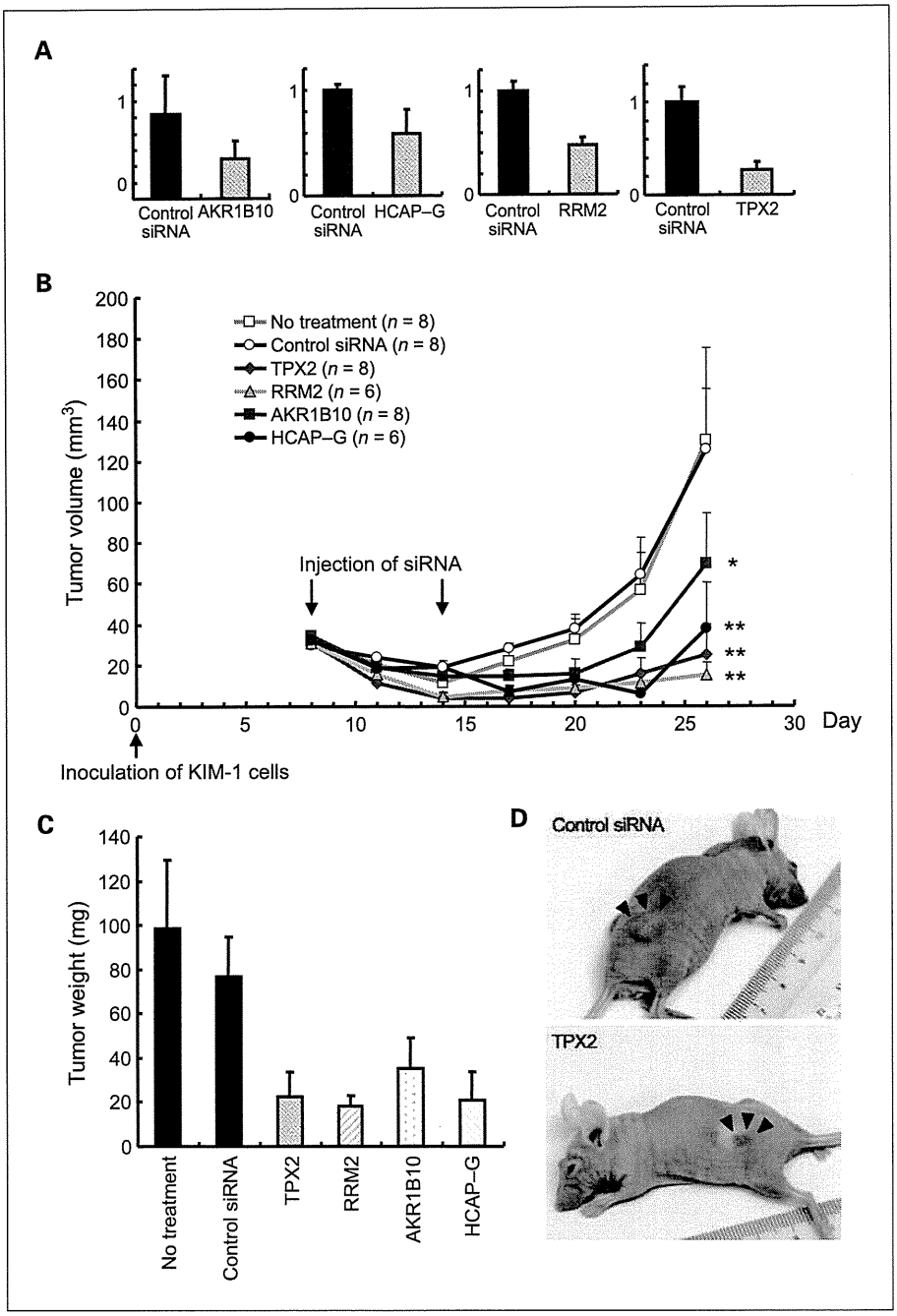

Fig. 6. Suppression of tumor growth by siRNA. A, KIM-1 cells were s.c. inoculated into the flanks of nude mice. Eight days later, control siRNA or siRNA against *AKR1B10, HCAP-G, RRM2*, or *TPX2* was injected into the developed tumors. The tumors were excised 2 days after the injection, and the expression levels of the indicated genes were determined by real-time PCR. Values of control siRNA were set at 1. B, chronological changes in tumor volume after two injections of the indicated siRNA. Volume of tumors was determined every 3 days as described in Materials and Methods. **, significantly different with a Bonferroni-corrected *P* value of <0.001. *, significantly different with a Bonferroni-corrected *P* value of 0.012. C, weight (mean + SE in mg) of xenografts measured 18 days after the second injection of the indicated siRNA and controls. D, macroscopic appearance of xenografts injected with control siRNA (top) and siRNA against TPX2 (bottom).

although the four selected genes seem to be highly relevant from a biological viewpoint. HCC has been recognized as a single category of disease; however, the overall gene expression patterns seem to differ markedly among individual cases. A search for the genes responsible for the different clinical outcomes of HCC will be the subject of a future study. We used the cell proliferation assay for siRNA-based functional screening. However, the use of other assays capable of evaluating cell motility, migration, drug sensitivity, or cell death may help to identify genes differing in their biological significance. The combination of genome-wide expression and functional screening described here provides a rapid and comprehensive approach that could be applicable for studies of various aspects of human cancer.

Disclosure of Potential Conflicts of Interest

No potential conflicts of interest were disclosed.

Acknowledgments

We thank Dr. Masamichi Kojiro (Kurume University, Kurume, Japan) for providing the KIM-1 cells.

Grant Support

Program for Promotion of Fundamental Studies in Health Sciences conducted by the National Institute of Biomedical Innovation of Japan, the Third-Term Comprehensive Control Research for Cancer conducted by the Ministry of Health, Labor and Welfare of Japan, and generous grants from the Natio Foundation and the Princess Takamatsu Cancer Research Fund. These fund resources did not influence the study design or interpretation of the results.

The costs of publication of this article were defrayed in part by the payment of page charges. This article must therefore be hereby marked *advertisement* in accordance with 18 U.S.C. Section 1734 solely to indicate this fact.

Received 08/15/2009; revised 02/01/2010; accepted 03/08/2010; published OnlineFirst 04/13/2010.

References

1. El-Serag HB, Rudolph KL. Hepatocellular carcinoma: epidemiology and molecular carcinogenesis. Gastroenterology 2007;132:2557–76.
2. Hernandez-Boluda JC, Cervantes F. Imatinib mesylate (Gleevec, Glivec):a new therapy for chronic myeloid leukemia and other malignancies. Drugs Today (Barc) 2002;38:601–13.
3. Fong T, Morgensztern D, Govindan R. EGFR inhibitors as first-line therapy in advanced non-small cell lung cancer. J Thorac Oncol 2008;3:303–10.
4. Llovet JM, Ricci S, Mazzaferro V, et al. Sorafenib in advanced hepatocellular carcinoma. N Engl J Med 2008;359:378–90.
5. Di Maio M, Daniele B, Perrone F. Targeted therapies: role of sorafenib in HCC patients with compromised liver function. Nat Rev Clin Oncol 2009;6:505–6.
6. Hideshima T, Chauhan D, Richardson P, Anderson KC. Identification and validation of novel therapeutic targets for multiple myeloma. J Clin Oncol 2005;23:6345–50.
7. Izzo F, Marra P, Beneduce G, et al. Pegylated arginine deiminase treatment of patients with unresectable hepatocellular carcinoma: results from phase I/II studies. J Clin Oncol 2004;22:1815–22.
8. Drew Y, Plummer R. The emerging potential of poly(ADP-ribose) polymerase inhibitors in the treatment of breast cancer. Curr Opin Obstet Gynecol 2010;22:67–71.
9. Whitehurst AW, Bodemann BO, Cardenas J, et al. Synthetic lethal screen identification of chemosensitizer loci in cancer cells. Nature 2007;446:815–9.
10. Silva JM, Marran K, Parker JS, et al. Profiling essential genes in human mammary cells by multiplex RNAi screening. Science 2008;319:617–20.
11. Schlabach MR, Luo J, Solimini NL, et al. Cancer proliferation gene discovery through functional genomics. Science 2008;319:620–4.
12. Luo B, Cheung HW, Subramanian A, et al. Highly parallel identification of essential genes in cancer cells. Proc Natl Acad Sci U S A 2008;105:20380–5.
13. Huang L, Shitashige M, Satow R, et al. Functional interaction of DNA topoisomerase IIα with the β-catenin and T-cell factor-4 complex. Gastroenterology 2007;133:1569–78.
14. Shitashige M, Naishiro Y, Idogawa M, et al. Involvement of splicing factor-1 in β-catenin/T-cell factor-4-mediated gene transactivation and pre-mRNA splicing. Gastroenterology 2007;132:1039–54.
15. Honda K, Yamada T, Hayashida Y, et al. Actinin-4 increases cell motility and promotes lymph node metastasis of colorectal cancer. Gastroenterology 2005;128:51–62.
16. Yamaguchi U, Nakayama R, Honda K, et al. Distinct gene expression-defined classes of gastrointestinal stromal tumor. J Clin Oncol 2008;26:4100–8.
17. Minakuchi Y, Takeshita F, Kosaka N, et al. Atelocollagen-mediated synthetic small interfering RNA delivery for effective gene silencing *in vitro* and *in vivo*. Nucleic Acids Res 2004;32:e109.
18. Takeshita F, Minakuchi Y, Nagahara S, et al. Efficient delivery of small interfering RNA to bone-metastatic tumors by using atelocollagen *in vivo*. Proc Natl Acad Sci U S A 2005;102:12177–82.
19. Shi L, Reid LH, Jones WD, et al. The MicroArray Quality Control (MAQC) project shows inter- and intraplatform reproducibility of gene expression measurements. Nat Biotechnol 2006;24:1151–61.
20. Bolker BM, Brooks ME, Clark CJ, et al. Generalized linear mixed models: a practical guide for ecology and evolution. Trends Ecol Evol 2009;24:127–35.
21. Gardina PJ, Clark TA, Shimada B, et al. Alternative splicing and differential gene expression in colon cancer detected by a whole genome exon array. BMC Genomics 2006;7:325.
22. Hussain SP, Schwank J, Staib F, Wang XW, Harris CC. TP53 mutations and hepatocellular carcinoma: insights into the etiology and pathogenesis of liver cancer. Oncogene 2007;26:2166–76.
23. Gouas D, Shi H, Hainaut P. The aflatoxin-induced TP53 mutation at codon 249 (R249S): biomarker of exposure, early detection and target for therapy. Cancer Lett 2009;286:29–37.
24. Villanueva A, Newell P, Chiang DY, Friedman SL, Llovet JM. Genomics and signaling pathways in hepatocellular carcinoma. Semin Liver Dis 2007;27:55–76.
25. Katoh H, Shibata T, Kokubu A, et al. Genetic inactivation of the APC gene contributes to the malignant progression of sporadic hepatocellular carcinoma: a case report. Genes Chromosomes Cancer 2006;45:1050–7.
26. Shao J, Zhou B, Chu B, Yen Y. Ribonucleotide reductase inhibitors and future drug design. Curr Cancer Drug Targets 2006;6:409–31.
27. Gruss OJ, Vernos I. The mechanism of spindle assembly: functions of Ran and its target TPX2. J Cell Biol 2004;166:949–55.
28. Bayliss R, Sardon T, Ebert J, Lindner D, Vernos I, Conti E. Determinants for Aurora-A activation and Aurora-B discrimination by TPX2. Cell Cycle 2004;3:404–7.
29. Marumoto T, Zhang D, Saya H. Aurora-A—a guardian of poles. Nat Rev Cancer 2005;5:42–50.
30. Keen N, Taylor S. Aurora-kinase inhibitors as anticancer agents. Nat Rev Cancer 2004;4:927–36.
31. Harrington EA, Bebbington D, Moore J, et al. VX-680, a potent and selective small-molecule inhibitor of the Aurora kinases, suppresses tumor growth *in vivo*. Nat Med 2004;10:262–7.
32. Anderson K, Yang J, Koretke K, et al. Binding of TPX2 to Aurora A alters substrate and inhibitor interactions. Biochemistry 2007;46:10287–95.
33. Gerlich D, Hirota T, Koch B, Peters JM, Ellenberg J. Condensin I stabilizes chromosomes mechanically through a dynamic interaction in live cells. Curr Biol 2006;16:333–44.
34. Lam WW, Peterson EA, Yeung M, Lavoie BD. Condensin is required for chromosome arm cohesion during mitosis. Genes Dev 2006;20:2973–84.
35. Scuric Z, Stain SC, Anderson WF, Hwang JJ. New member of aldose reductase family proteins overexpressed in human hepatocellular carcinoma. Hepatology 1998;27:943–50.
36. Teramoto R, Minagawa H, Honda M, et al. Protein expression profile characteristic to hepatocellular carcinoma revealed by 2D-DIGE with supervised learning. Biochim Biophys Acta 2008;1784:764–72.
37. Li CP, Goto A, Watanabe A, et al. AKR1B10 in usual interstitial pneumonia: expression in squamous metaplasia in association with smoking and lung cancer. Pathol Res Pract 2008;204:295–304.

Supplementary Table S1. Clinicopathological characteristics of HCC patients

	Discovery Set 1	Discovery Set 2	Validation Set 1	Validation Set 2
Total no. of patients	10	10	20	44
Age, years				
Mean (SD)	66.1 (5.9)	68 (8.9)	61.3 (10.9)	64.8 (9.9)
Sex, no. of patients (%)				
Male	10	9	16 (80)	35 (79.5)
Female	0	1	4 (20)	9 (20.5)
Hepatitis virus infection, no. of patients (%)				
No	1	1	2 (10)	9 (20.5)
B	2	5	7 (35)	12 (27.3)
C	6	3	11 (55)	20 (45.5)
B+C	1	1	0	3 (6.8)
Background liver, no. of patients (%)				
Normal	0	0	1 (5)	5 (11.4)
Chronic hepatitis (CH)	7	3	8 (40)	23 (52.3)
Liver cirrhosis (LC)	2	4	8 (40)	8 (18.2)
CH + LC	0	0	1 (5)	0
Precirrhosis	1	3	2 (10)	8 (18.2)
Tumor size, cm3				
mean (SD)	68.3 (42.0)	120.9 (218.1)	87.8 (111.9)	176.4 (256.7)
Histology, no. of patients (%)				
Well	1	0	1 (5)	5 (11.4)
Well to moderately	0	0	4 (20)	0
Moderately	5	10	8 (40)	27 (61.4)
Moderately to poorly	1	0	1 (5)	0
Poorly	3	0	6 (30)	12 (27.3)
Intrahepatic metastases, no. of patients (%)				
0	7	7	17 (85)	30 (68.2)
1	1	1	2 (10)	14 (31.8)
2	2	2	0	0
3	0	0	1 (5)	0
Portal vein involvement, no. of patients (%)				
0	4	1	10 (50)	17 (38.6)
1	5	8	7 (35)	24 (54.5)
2	0	1	0	1 (2.3)
3	1	0	3 (15)	2 (4.5)

Supplementary Table S2. List of genes up-regulated in HCC (Discovery Set 1)

Transcript Cluster ID	RefSeq	Gene symbol	*P*-value	Fold change	Gene description
2337716	NM_006252	PRKAA2	6.71E-04	4.42	Protein kinase, AMP-activated, alpha 2 catalytic subunit
2379863	NM_016343	CENPF|TUBD1|PAK1	1.05E-04	3.22	Centromere protein F, 350/400ka (mitosin) | tubulin, delta 1 | p21/Cdc42/Rac1-activated kinase 1 (STE20 homolog, yeast)
2427007	NM_002959	SORT1|PSRC1|MYBPHL	1.24E-04	3.14	Sortilin 1 | proline/serine-rich coiled-coil 1 | myosin binding protein H-like
2441386	NM_003617	RGS5|UPK1B	5.06E-06	3.27	Regulator of G-protein signalling 5 | uroplakin 1B
2449559	NM_018136	ASPM	4.37E-05	3.03	Asp (abnormal spindle) homolog, microcephaly associated (Drosophila)
2469252	NM_001034	RRM2	6.68E-06	3.36	Ribonucleotide reductase M2 polypeptide
2544201	NM_004881|NM_147184	TP53I3|PFN4	7.69E-06	3.67	Tumor protein p53 inducible protein 3 | profilin family, member 4
2784113	NM_001237	CCNA2	4.01E-04	3.43	Cyclin A2
2813414	NM_031966	CCNB1	5.02E-06	3.53	Cyclin B1
2899102	NM_003531	HIST1H3C	5.21E-05	4.94	Histone cluster 1, H3c
2946215	NM_003537	HIST1H3B	3.73E-06	4.99	Histone cluster 1, H3b
2947077	NM_003533	HIST1H3I	2.49E-05	3.61	Histone cluster 1, H3i
2997376	NM_018685	ANLN	1.43E-05	3.39	Anillin, actin binding protein
3025433	NM_020299	AKR1B10|LOC340888|LOC441282	4.50E-04	18.03	Aldo-keto reductase family 1, member B10 (aldose reductase) | similar to aldo-keto reductase family 1, member B10
3260586	NM_005063	SCD|LOC645313|LOC651109	8.76E-05	3.43	Stearoyl-CoA desaturase (delta-9-desaturase) | similar to Acyl-CoA desaturase (Stearoyl-CoA desaturase) (Fatty acid desaturase) (Delta(9)-desaturase)
3329343	NM_002391|NM_001012334|NM_001012333	MDK	4.38E-04	3.90	Midkine (neurite growth-promoting factor 2)
3375545	NM_013402	FADS1|FADS3	2.74E-04	3.34	Fatty acid desaturase 1 | fatty acid desaturase 3
3590388	NM_018454|NM_016359	NUSAP1	1.62E-05	3.09	Nucleolar and spindle associated protein 1
3756193	NM_001067	TOP2A	7.29E-06	4.63	Topoisomerase (DNA) II alpha 170kDa
3881443	NM_012112	TPX2|TINAGL1	2.10E-06	3.11	TPX2, microtubule-associated, homolog (Xenopus laevis) | tubulointerstitial nephritis antigen-like 1
3639031	NM_199414|NM_199413|NM_003981	PRC1	8.32E-06	3.17	Protein regulator of cytokinesis 1

Supplementary Table S3. List of genes down-regulated in HCC (Discovery Set 1)

Transcript Cluster ID	RefSeq	Gene symbol	*P*-value	Fold change	Gene description
2331679	NM_032793	MFSD2|LOC731362	1.37E-05	3.98	Major facilitator superfamily domain containing 2 | similar to ribosomal protein S2
2337786	NM_000562	C8A	6.13E-04	3.77	Complement component 8, alpha polypeptide
2377332	NM_000651|NM_000573	CR1|LOC653907	3.69E-08	3.32	Complement component (3b/4b) receptor 1 (Knops blood group) | similar to complement component (3b/4b) receptor 1 isoform F precursor
2388085	NM_003679	KMO	2.13E-04	3.96	Kynurenine 3-monooxygenase (kynurenine 3-hydroxylase)
2403080	NM_003665|NM_173452	MAP3K6|FCN3	4.00E-09	18.47	Mitogen-activated protein kinase kinase kinase 6 | ficolin (collagen/fibrinogen domain containing) 3 (Hakata antigen)
2439138	NM_005894	CD5L	1.52E-06	12.18	CD5 molecule-like
2443120	NM_001937	DPT	4.15E-07	5.63	Dermatopontin
2475911	NM_014600	EHD3	3.24E-09	3.30	EH-domain containing 3
2502686	NM_006770	MARCO	8.19E-10	6.79	Macrophage receptor with collagenous structure
2547231	NM_000348	SRD5A2	7.70E-05	4.20	Steroid-5-alpha-reductase, alpha polypeptide 2 (3-oxo-5 alpha-steroid delta 4-dehydrogenase alpha 2)
2678298	NM_004944	DNASE1L3|ACTB	5.72E-07	9.65	Deoxyribonuclease I-like 3 | actin, beta
2693620	NM_144639	UROC1	2.30E-06	6.38	Urocanase domain containing 1
2716124	NM_001528	HGFAC	9.54E-07	4.84	HGF activator
2729852	NM_005953	MT2A|MT1M|LOC441019|NUTF2	1.53E-04	3.38	Metallothionein 2A | metallothionein 1M | hypothetical gene supported by X97260; BC070289 | nuclear transport factor 2
2745899	NM_022475	HHIP	7.34E-08	3.97	Hedgehog interacting protein
2772566	NM_144646	IGJ	4.02E-04	7.76	Immunoglobulin J polypeptide, linker protein for immunoglobulin alpha and mu polypeptides
2773434	NM_002089	CXCL2	1.94E-05	5.90	Chemokine (C-X-C motif) ligand 2
2775259	NM_152545	RASGEF1B|ALK|RBM41	6.25E-05	3.25	RasGEF domain family, member 1B | anaplastic lymphoma kinase (Ki-1) | RNA binding motif protein 41
2775390		MOP-1	8.90E-04	3.53	
2775909	NM_016619	PLAC8	7.54E-11	13.74	Placenta-specific 8
2792127	NM_000909	NPY1R|LOC729743|LOC731120	6.08E-09	3.06	Neuropeptide Y receptor Y1 | similar to neuropeptide Y receptor Y1
2794584	NM_005277|NM_201591|NM_201592	GPM6A|MPDU1	9.68E-09	3.47	Glycoprotein M6A | mannose-P-dolichol utilization defect 1
2807716	NM_000587	C7	2.60E-05	11.43	Complement component 7
2816536	NM_001882	CRHBP	3.45E-09	13.85	Corticotropin releasing hormone binding protein
2842624	NM_017675	PCLKC	6.73E-04	4.88	Protocadherin LKC
2853055	NM_031900	AGXT2	4.55E-04	3.61	Alanine-glyoxylate aminotransferase 2
2854092	NM_002310	LIFR	2.95E-07	7.18	Leukemia inhibitory factor receptor alpha
2854409	NM_001737	C9|ASTN2	7.35E-05	16.46	Complement component 9 | astrotactin 2
2876608	NM_004887	CXCL14	8.13E-08	4.89	Chemokine (C-X-C motif) ligand 14
2883283	NM_138379	TIMD4	3.38E-08	4.36	T-cell immunoglobulin and mucin domain containing 4
2907513	NM_018960	GNMT	1.61E-04	6.98	Glycine N-methyltransferase
2955761	NM_016593	CYP39A1	6.59E-04	3.97	Cytochrome P450, family 39, subfamily A, polypeptide 1
2975257	NM_022568|NM_170771	ALDH8A1|HBS1L	7.13E-04	3.41	Aldehyde dehydrogenase 8 family, member A1 | HBS1-like (S. cerevisiae)
2982630	NM_024492|NM_145727	LPAL2|LOC732058|PLGLB2	5.06E-05	3.86	Lipoprotein, Lp(a)-like 2 | similar to Apolipoprotein(a) precursor (Apo(a)) (Lp(a)) | plasminogen-like B2
2982730	NM_005577	LPA|LOC732390|LOC732436|PLGLB2|TMEM166	8.05E-06	7.98	Llipoprotein, Lp(a) | similar to Apolipoprotein(a) precursor (Apo(a)) (Lp(a)) | plasminogen-like B2 | transmembrane protein 166

2995476		INMT	1.51E-05	3.47	Indolethylamine N-methyltransferase
3049292	NM_001013398|NM_000598	IGFBP3	4.56E-05	4.96	Insulin-like growth factor binding protein 3
3058944	NM_001010932|NM_000601|NM_001010931|NM_001010933|NM_001010934	HGF	1.38E-05	5.69	Hepatocyte growth factor (hepapoietin A; scatter factor)
3060332	NM_024636	STEAP4	5.41E-06	3.70	STEAP family member 4
3065740	NM_173054|NM_005045	RELN	3.74E-04	5.62	Reelin
3095257	NM_194294	INDOL1	2.39E-04	3.08	Indoleamine-pyrrole 2,3 dioxygenase-like 1
3095313	NM_020130	C8orf4	1.82E-07	3.76	Chromosome 8 open reading frame 4
3113133	NM_006438	COLEC10	1.37E-06	13.60	Collectin sub-family member 10 (C-type lectin)
3128817	NM_000680|NM_033303|NM_033304|NM_033302	ADRA1A	1.87E-04	3.71	Adrenergic, alpha-1A-, receptor
3193631	NM_004108|NM_015837	FCN2	1.70E-07	3.64	Ficolin (collagen/fibrinogen domain containing lectin) 2 (hucolin)
3204285	NM_006274	CCL19	4.46E-05	11.65	Chemokine (C-C motif) ligand 19
3204301	NM_002989	CCL21	1.51E-04	4.04	Chemokine (C-C motif) ligand 21
3215570	NM_000507	FBP1	2.86E-04	3.65	Fructose-1,6-bisphosphatase 1
3237286	NM_001009567	MRC1	1.08E-06	4.72	Mannose receptor, C type 1
3251566	NM_152635	OIT3|C1orf146	2.82E-08	10.95	Oncoprotein induced transcript 3 | chromosome 1 open reading frame 146
3286602	NM_000609|NM_199168|NM_001033886	CXCL12	3.57E-06	5.02	Chemokine (C-X-C motif) ligand 12 (stromal cell-derived factor 1)
3302533	NM_003015	SFRP5	1.38E-05	4.31	Secreted frizzled-related protein 5
3333811	NM_001039752	SLC22A10	3.50E-04	5.11	Solute carrier family 22 (organic anion/cation transporter), member 10
3348940	NM_031938|NM_001037290	KCTD9|BCDO2|LOC728291|LOC642513|LOC728707|LOC729404|LOC730942|LOC650978|LOC647852|LOC731540	3.85E-05	4.40	Potassium channel tetramerisation domain containing 9 | beta-carotene dioxygenase 2 | similar to potassium channel tetramerisation domain containing 9 | hypothetical protein LOC728707
3349858	NM_006169	NNMT	2.28E-05	9.79	Nicotinamide N-methyltransferase
3359121	NR_003512|NM_001007139|NM_000612	INS-IGF2	7.64E-04	13.10	Insulin- insulin-like growth factor 2 | insulin-like growth factor 2 (somatomedin A)
3360401	NM_000518	HBB	3.13E-06	3.35	Hemoglobin, beta
3362826	NM_006691	XLKD1	6.72E-09	8.65	Extracellular link domain containing 1
3365318	NM_006512	SAA4	9.90E-04	3.56	Serum amyloid A4, constitutive
3374934	NM_152852|NM_022349|NM_152851	MS4A6A|LOC643680	2.47E-05	3.25	Membrane-spanning 4-domains, subfamily A, member 6A | hypothetical protein
3402786	NM_000616	CD4|S100PBP	1.43E-06	3.07	CD4 molecule | S100P binding protein
3426257	NM_003877	SOCS2	6.46E-04	4.70	Suppressor of cytokine signaling 2
3428573	NM_152323	SPIC|LOC646120	2.74E-05	3.06	Spi-C transcription factor (Spi-1/PU.1 related) | similar to Spi-C transcription factor (Spi-1/PU.1 related)
3429159	NM_017564	STAB2	3.97E-09	9.37	Stabilin 2
3442706	NM_004244|NM_203416	CD163	9.19E-06	4.07	
3443936	NM_016509	CLEC1B	1.47E-10	6.14	C-type lectin domain family 1, member B
3457794	NM_001638	APOF|STAT2	7.09E-04	10.21	Apolipoprotein F | signal transducer and activator of transcription 2, 113kDa
3457891	NM_013267	GLS2	9.06E-06	8.54	Glutaminase 2 (liver, mitochondrial)
3465274	NM_001920|NM_133503|NM_133504|NM_133505|NM_133506|NM_133507	DCN	2.73E-05	8.72	Decorin

3466687	NM_002108	HAL	8.59E-04	4.82	Histidine ammonia-lyase
3468345	NM_000618	IGF1	9.19E-04	5.16	Insulin-like growth factor 1 (somatomedin C)
3472366	NM_006843	SDS	7.40E-05	11.63	Serine dehydratase
3486096	NM_207361	FREM2	3.91E-04	4.61	FRAS1 related extracellular matrix protein 2
3502475	NM_003891	PROZ	7.77E-05	3.30	Protein Z, vitamin K-dependent plasma glycoprotein
3544525	NM_005252	FOS	5.63E-04	5.88	V-fos FBJ murine osteosarcoma viral oncogene homolog
3565524	NM_000161|NM_001024024|NM_001024070|NM_001024071	GCH1|LOC202181	2.98E-06	3.49	GTP cyclohydrolase 1 (dopa-responsive dystonia) | hypothetical protein LOC202181
3642664	NM_000517	HBA2|HBA1	2.14E-05	3.01	Hemoglobin, alpha 2 | hemoglobin, alpha 1
3651478	NM_005622|NM_202000	ACSM3	2.19E-04	4.11	Acyl-CoA synthetase medium-chain family member 3
3661940	NM_020988|NM_138736	GNAO1	2.93E-05	5.01	Guanine nucleotide binding protein (G protein), alpha activating activity polypeptide O
3662139	NM_175617	MT1E|MT1M|MT1A|NUTF2	6.83E-04	7.58	Metallothionein 1E (functional) | metallothionein 1M | metallothionein 1A (functional) | nuclear transport factor 2
3662150	NM_176870	MT1M|MT1JP|NUTF2	6.55E-04	6.69	Metallothionein 1M | metallothionein 1J (pseudogene) | nuclear transport factor 2
3662158		C20orf127|MT1JP|NUTF2	5.85E-04	5.65	Chromosome 20 open reading frame 127 | metallothionein 1J (pseudogene) | nuclear transport factor 2
3662201	NM_005951|NM_005949|NM_001039954	MT1F|MT1H|LOC645745|LOC727730|MT1A|NUTF2	6.89E-04	6.17	Metallothionein 1F (functional) | metallothionein 1H | metallothionein 1H-like protein | similar to metallothionein 1H-like protein | metallothionein 1A (functional) | nuclear transport factor 2
3662247	NM_005952	MT1X|MT1A|NUTF2	3.34E-04	4.93	Metallothionein 1X | metallothionein 1A (functional) | nuclear transport factor 2
3662417	NM_000078	CETP	1.44E-07	6.67	Cholesteryl ester transfer protein, plasma
3667811	NM_001361	DHODH	5.29E-05	3.68	Dihydroorotate dehydrogenase
3692999	NM_005950	MT1G|NUTF2	8.51E-04	8.16	Metallothionein 1G | nuclear transport factor 2
3696035	NM_000229	LCAT	1.50E-05	3.98	Lecithin-cholesterol acyltransferase
3742627		UNQ5783	2.48E-07	3.26	DTFT5783
3748798	NM_002404	MFAP4	1.01E-05	4.91	Microfibrillar-associated protein 4
3768627	NM_007168	ABCA8	8.15E-04	3.23	ATP-binding cassette, sub-family A (ABC1), member 8
3793827	NM_032649	CNDP1	2.87E-05	4.19	Carnosine dipeptidase 1 (metallopeptidase M20 family)
3819130	NM_214677|NM_214678|NM_214679|NM_014257|NM_214676|NM_214675	CLEC4M	8.20E-09	13.16	C-type lectin domain family 4, member M
3830306	NM_021175	HAMP	8.23E-09	52.87	Hepcidin antimicrobial peptide
3848525	NM_198492	CLEC4G	6.15E-10	6.21	C-type lectin superfamily 4, member G
3881391	NM_181353|NM_002165	ID1	3.28E-06	6.01	Inhibitor of DNA binding 1, dominant negative helix-loop-helix protein
3883233		C20orf127|MT1JP|MT1M|MT1A	6.22E-04	5.41	Chromosome 20 open reading frame 127 | metallothionein 1J (pseudogene) | metallothionein 1M | metallothionein 1A (functional)
3890640	NM_002591	PCK1	9.83E-04	7.09	Phosphoenolpyruvate carboxykinase 1 (soluble)
3974019	NM_004615	TSPAN7	6.45E-04	3.16	Tetraspanin 7
4007164	NM_002621	CFP	5.21E-10	3.72	Complement factor properdin
4011008	NM_007268	EIF4B|VSIG4|LOC643873|LOC339881|LOC645430|LOC392485|LOC650271|THRSP	5.70E-05	3.50	Eukaryotic translation initiation factor 4B | V-set and immunoglobulin domain containing 4 | similar to eukaryotic translation initiation factor 4B | hypothetical LOC645430 | similar to ataxin 7-like 3 | hypothetical protein LOC650271 | thyroid hormone responsive (SPOT14 homolog, rat)
4020655	NM_014253	ODZ1	8.93E-04	3.60	Odz, odd Oz/ten-m homolog 1(Drosophila)
4027639	NM_000132|NM_019863	F8	1.69E-05	3.01	Coagulation factor VIII, procoagulant component (hemophilia A)

Supplementary Table S4. List of siRNA

Gene symbol	ID
AKR1B10	43766
	133050
	112090
ANLN	132619
	132620
	132621
CCNB1	118838
	118839
DEPDC1	148669
	148670
	148671
HCAP-G	125362
	125363
	125364
HIST1H3B	214117
	214118
	214119
HIST1H3C	13270
	45052
	44958
HIST1H3I	13272
	44960
	45054
RRM2	9302
	110819
	110822
TPX2	19774
	136425
	136426

Supplementary Table S5. List of TaqMan Gene Expression Assays

Gene symbol	Assay ID
AKR1B10	Hs00252524_m1
ANLN	Hs00218803_m1
C7	Hs00175109_m1
CCNA2	Hs00153138_m1
COLEC10	Hs00197571_m1
CRHBP	Hs00181810_m1
HAMP	Hs00221783_m1
HCAP-G	Hs00254617_m1
HIST1H3I	Hs00605800_s1
RGS5	Hs00186212_m1
RRM2	Hs00357247_g1
TPX2	Hs00201616_m1

Supplementary Table S6. Effects of siRNA treatment on the growth of xenografts

	Estimate*	Standard error*	*t*-Value	Adjusted *P*-value
Control (Intercept)	3.744	0.189		
TPX2	-1.239	0.161	-7.699	< 0.001
RRM2	-1.153	0.168	-6.878	< 0.001
AKR	-0.499	0.162	-3.088	0.012
HCAPG	-0.782	0.168	-4.667	< 0.001

*On a natural logarithmic scale.

Annals of Oncology 24: 84–90, 2013
doi:10.1093/annonc/mds215
Published online 10 August 2012

Diagnostic and prognostic significance of the alternatively spliced *ACTN4* variant in high-grade neuroendocrine pulmonary tumours

A. Miyanaga[1,2], K. Honda[1], K. Tsuta[3], M. Masuda[1], U. Yamaguchi[1], G. Fujii[4], A. Miyamoto[5], S. Shinagawa[5], N. Miura[1], H. Tsuda[3], T. Sakuma[6], H. Asamura[7], A. Gemma[2] & T. Yamada[1]*

[1]*Division of Chemotherapy and Clinical Research, National Cancer Center Research Institute, Tokyo;* [2]*Department of Internal Medicine, Division of Pulmonary Medicine, Infection and Oncology, Nippon Medical School, Tokyo;* [3]*Division of Pathology and Clinical Laboratories, National Cancer Center Hospital, Tokyo;* [4]*Division of Cancer Prevention Research, National Cancer Center Research Institute, Tokyo ;* [5]*Kobe Research Center, TransGenic Inc., Kumamoto;* [6]*BioBusiness Group, Mitsui Knowledge Industry, Tokyo;* [7]*Division of Thoracic Surgery, National Cancer Center Hospital, Tokyo, Japan*

Received 2 April 2012; revised 30 May 2012; accepted 31 May 2012

Background: High-grade neuroendocrine tumours (HGNTs) of the lung manifest a wide spectrum of clinical behaviour, but no method for predicting their outcome has been established.
Materials and methods: We newly established a monoclonal antibody specifically recognizing the product of the alternatively spliced *ACTN4* transcript (namely, variant actinin-4), and used it to examine the expression of variant actinin-4 immunohistochemically in a total of 609 surgical specimens of various histological subtypes of lung cancer.
Results: Variant actinin-4 was expressed in 55% (96/176) of HGNTs, but in only 0.8% (3/378) of non-neuroendocrine (NE) lung cancers. The expression of variant actinin-4 was significantly associated with poorer overall survival in HGNT patients ($P = 0.00021$, log-rank test). Multivariate analysis using the Cox proportional hazards model showed that the expression of variant actinin-4 was the most significant independent negative predictor of survival in HGNT patients (hazard ratio (HR), 2.15; $P = 0.00113$) after the presence of lymph node metastasis (HR, 2.25; $P = 0.00023$).
Conclusions: The expression of variant actinin-4 is an independent prognostic factor for patients with HGNTs. This protein has a high affinity for filamentous actin polymers and likely promotes aggressive behaviour of cancer cells. The present clinical findings clearly support this notion.
Key words: actinin-4, alternative splice variant, diagnostic marker, high-grade neuroendocrine tumour, pulmonary neoplasm, prognosis

introduction

Neuroendocrine (NE) tumours comprise 20%–25% of all human lung malignancies and are classified into four histological subtypes: typical carcinoid (TC), atypical carcinoid (AC), large cell neuroendocrine carcinoma (LCNEC) and small cell lung carcinoma (SCLC) [1, 2]. TC and AC are tumours with low- to intermediate-grade malignancy, whereas LCNEC and SCLC are highly aggressive and collectively referred to as high-grade neuroendocrine tumours (HGNTs) [3–6].

LCNEC appeared in the World Health Organization (WHO) Histological Typing of Lung and Pleural Tumours (third version, 1999) as a new entity of large cell carcinoma [2]. LCNEC shows aggressive behaviour distinct from other non-small cell lung cancers (NSCLCs) [7], and thus its accurate discrimination is essential for the management of lung cancer patients. TC, AC and SCLC can be readily diagnosed on the basis of their histological characteristics, but the diagnosis of LCNEC is more complicated. The morphological features of NE differentiation are often inconspicuous, especially in small biopsy or cytology specimens [2].

Three NE markers are used routinely for immunohistochemical assessment of NE differentiation: neural cell adhesion molecule (CD56), chromogranin A (CGA) and synaptophysin (SYN). However, a significant proportion of LCNECs are negative for any of these NE markers [7], and more problematically, some non-NE lung cancers also show equivocal immunoreactivity for these markers [7, 8]. Therefore, it is necessary to develop a new diagnostic biomarker with higher specificity.

Actinin-4 is an actin-binding protein that we originally identified as being associated with enhanced cell motility and cancer invasion [9]. The actinin-4 (*ACTN4*) gene has a unique structure (supplementary Figure S1, available at *Annals of*

Correspondence to: Prof. T. Yamada, Division of Chemotherapy and Clinical Research, National Cancer Center Research Institute, 5-1-1 Tsukiji, Chuo-ku, Tokyo 104-0045, Japan. Tel: +81-3-3542-2511; Fax: +81-3-3547-6045; E-mail: tyamada@ncc.go.jp

Oncology online), possessing two exons 8 (8 and 8?) of the same size, the mutually exclusive use of which leads to the production of two kinds of mRNA. The transcript obtained with exon 8 is expressed ubiquitously (namely, the ubiquitous form or *ACTN4*-Ub), whereas the expression of the variant transcript obtained with exon 8? (the variant form or *ACTN4*-Va) is undetectable in normal tissues except for testis and brain [10, 11]. We previously found that the variant transcript is frequently expressed in SCLCs and that the gene product can be categorized as a so-called cancer-testis antigen [10]. However, the clinical significance of variant actinin-4 has remained undetermined due to lack of a specific probe.

The alternatively spliced actinin-4 variant transcript is predicted to encode a polypeptide differing in only three amino acids. To produce an antibody that can detect this small difference, we used the *GANP* (germinal centre-associated nuclear protein) technology [12]. *GANP* transgenic mice generate a highly diverse spectrum of antibodies and have been used to produce high-affinity antibodies against various difficult antigens, such as those with small protein modifications [13]. Here, we report the establishment of a highly specific antibody recognizing variant actinin-4 protein and the potential utility of variant actinin-4 not only as a new diagnostic biomarker but also as a highly potent prognostic biomarker for HGNTs.

materials and methods

cell lines and sequencing

Total RNA was extracted from 91 human cancer cell lines (31 lung cancers, 23 colorectal cancers, 7 stomach cancers, 5 hepatocellular carcinomas, 6 pancreatic cancers, 4 choriocarcinomas, 4 ovary cancers, 4 oral cancers, 3 prostate cancers, 2 breast cancers, 1 bladder cancer and 1 cervical cancer) using TRIzol reagent (Life Technologies, Grand Island, NY) (supplementary Table S1, available at *Annals of Oncology* online).

First-strand complementary DNA (cDNA) was synthesized in the presence of random primers using the high-capacity cDNA reverse transcription kit (Life Technologies) in accordance with the manufacturer's instructions. The entire coding region of *ACTN4* was amplified and sequenced using the BigDye Terminator v3.1 Cycle Sequencing Ready Reaction Kit (Life Technologies).

production of monoclonal antibodies

GANP transgenic mice were immunized with a synthetic peptide (NQSYQYGPSSAGNGAG) to produce a monoclonal antibody (namely 13G9) reactive with all the known forms (ubiquitous and variant) of actinin-4. Another monoclonal antibody specific to variant actinin-4 (namely 15H2) was raised against a synthetic peptide (DIVGTLRPDEKAIMTYVSC). The reactivity and titre of antibodies against the various peptides were assessed by the antibody capture assay as described previously [13].

western blot analysis

The PCR-amplified fragments encoding the ubiquitous and variant forms of actinin-4 (amino acids 28–911) were cloned into the EcoRI and KpnI sites of the pEGFP-C1 vector (Takara Bio, Otsu, Japan) to express the ubiquitous and variant actinin-4 proteins fused with green fluorescent protein (GFP) at the N-termini (namely pEGFP-ACTN4-Ub and pEGFP-ACTN4-Va, respectively). The nucleotide sequences of all the PCR-amplified fragments were verified by sequencing. HEK293 cells (Health Science Research Resources Bank, Osaka, Japan) were transfected with each plasmid using Lipofectamine 2000 reagent (Life Technologies).

Western blotting was carried out following standard procedures, as described previously [14, 15]. Cells were extracted with lysis buffer [10 mmol/l HEPES (pH 7.4), 150 mmol/l NaCl, 1 mmol/l EDTA, 1% Triton X-100, 1% NP40 and 1 mg/ml NaN_3] containing a protease inhibitor cocktail (Sigma-Aldrich, St. Louis, MO) on ice for 30 min. Ten micrograms of cell lysate were reduced, denatured at 70°C for 10 min and fractionated through NuPAGE 4%–12% Bis-Tris gel (Life Technologies). The fractionated proteins were then blotted onto PVDF membranes (Life Technologies). After incubation with the primary antibody at 4°C overnight, the blots were incubated with appropriate horseradish peroxidase-linked secondary antibodies and then detected by enhanced chemiluminescence (Western Lightning ECL Pro; Perkin-Elmer, Waltham, MA).

patients and tissue samples

Thirty-one tissue microarrays (TMAs) were constructed from formalin-fixed paraffin-embedded tissue blocks of 609 primary lung tumours that had been surgically resected at the National Cancer Center (NCC) Hospital (Tokyo, Japan) from 1982 to 2010 using a tissue-arraying instrument (KIN-1; Azumaya, Tokyo, Japan). Based on the Pathology and genetics of Tumours of the Lung, Pleura, Thymus and Heart [IARC (International Agency for Research on Cancer) WHO Classification of Tumours] (2004) [16], the 609 tumours were classified into carcinoid (51 cases), SCLC (70 cases), LCNEC (106 cases), adenocarcinoma (164 cases), squamous cell carcinoma (166 cases) and other NSCLCs (52 cases). To reduce sampling bias due to tissue heterogeneity, we took duplicate core samples measuring 2.0 mm in diameter from two different areas of every tumour.

The 176 patients with HGNTs included 143 men and 33 women with a mean age of 66 years (19–84 years). One hundred and sixty-nine (96%) patients had a history of habitual cigarette smoking. The follow-up periods ranged from 1 to 286 months (median follow-up, 46 months). Patients were staged postsurgically into IA (52 cases), IB (25 cases), IIA (33 cases), IIB (16 cases), IIIA (37 cases), IIIB (7 cases) and IV (6 cases) according to the International Union against Cancer (UICC) TNM classification of malignant tumours (7th edition, 2010) [17].

This study was conducted with approval from the Institutional Review Board of the NCC.

immunohistochemistry

TMA blocks were then cut into 4-mm thick sections and subjected to immunohistochemistry (IHC). Immunostaining of actinin-4 proteins was carried out using the Ventana DABMap detection kit and an automated slide stainer (Discovery XT, Ventana Medical Systems, Tucson, AZ) [18, 19]. Immunoreactivity was classified as positive when ≥10% of cancer cells showed cytoplasmic or membrane staining detectable at a magnification of ×40 [20, 21].

Deparaffinized TMA slides were incubated with anti-CD56 mouse monoclonal (1B6, Novocastra, Newcastle upon Tyne, UK), anti-CGA rabbit polyclonal (Dako, Glostrup, Denmark) or anti-SYN mouse monoclonal (27G12, Nichirei Biosciences, Tokyo, Japan) antibody for 1 h at room temperature. Immunoreactivity was detected with the EnVision plus kit (Dako) using 3, 3?-diaminobenzidine as the chromogen. For diagnosis of LCNEC, positive staining for at least one of the three NE markers was stipulated.

The results of IHC were judged by two investigators (AM and KT) who were blinded to any clinicopathological information, and any discrepancy in judgement was discussed.

statistical analysis

Overall survival was measured as the period from surgery to the date of death or last follow-up. Progression-free survival was defined as the length of time from surgery to the first detection of new lesions or death. Overall and progression-free survival was estimated by the Kaplan–Meier method using the StatFlex statistical software package (version 5.0, Artiteck, Osaka, Japan). Differences between the survival curves were assessed with the log-rank test. Univariate and multivariate analyses were carried out using the Cox regression model. Other statistical tests were carried out using tools available in the R statistical package (version 2.12.0; http://www.r-project.org/). Differences were considered to be statistically significant at $P < 0.05$.

results

expression of the *ACTN4* splice variant in cancer cell lines

We sequenced the entire coding region of the *ACTN4* transcript in 91 cell lines derived from human cancers of various origins (supplementary Table S1, available at *Annals of Oncology* online). No non-synonymous nucleotide substitution was detected except for those registered in the single nucleotide polymorphism database (http://www.ncbi.nlm.nih.gov/snp), indicating that somatic mutation of the *ACTN4* gene is infrequent. However, we detected overlap of two sequences appearing in nucleotides 793–872 of the *ACTN4* transcript (NM_004924.2) (supplementary Figure S2A, available at *Annals of Oncology* online) in 25% (23/91) of the cell lines. These two transcripts were separately cloned, and their nucleotide sequences were confirmed to be identical to the ubiquitous and variant transcripts of *ACTN4* that we had described previously [10] (supplementary Figure S2B, available at *Annals of Oncology* online).

The ubiquitous form of the *ACTN4* transcript (namely *ACTN4*-Ub) was expressed in all of the 91 human cancer cell lines examined, but the variant form (namely *ACTN4*-Va) was detected in 90% (18/20) of the SCLC cell lines examined (SBC-3, SBC-5, MS-1-L, Lu-135, Lu-143, STC-1, Lu-138, Lu-140, DMS153, DMS53, H1688, Wa-hT, H69AR, RERF-LCMS, Lu165, H69, Lu134-AH, Lu134-B, Lu-141 and Lu-139) and 25% (1/4) of the cell lines derived from pulmonary carcinoid tumour (NCI-H727, NCI-H835, UMC-11 and NCI-H720) (supplementary Table S1, available at *Annals of Oncology* online). In addition, the variant *ACTN4* mRNA was detected in 33% (1/3) of prostate cancers and 75% (3/4) of choriocarcinoma cell lines. However, none of the seven non-SCLC-derived cell lines examined (A549, PC9, LCD, LCKJ, LK-2, Lu-65 and Lu-99) expressed the variant transcript.

production of antibody specific to variant actinin-4 protein

Although there was a difference of only three amino acid residues between the ubiquitous and variant actinin-4 protein sequences deduced from their cDNA sequences (supplementary Figure S2C, available at *Annals of Oncology* online), we were able to produce a monoclonal antibody (15H2) that reacted specifically with a peptide for which the amino acid sequence was derived from the variant actinin-4 protein (DIVGTLRPDEKAIMTYVSC), but not with the corresponding sequence of the ubiquitous protein (DIVNTARPDEKAIMTYVSS) (underlining indicates the amino acids that differed) (Figure 1A).

To further confirm that the 15H2 monoclonal antibody reacted specifically with the variant form of actinin-4 protein, HEK 293 cells were transfected with a plasmid encoding the ubiquitous (pEGFP-ACTN4-Ub) or variant (pEGFP-ACTN4-Va) form of actinin-4. We found that the 15H2 antibody reacted only with a lysate prepared from HEK 293 cells transfected with pEGFP-ACTN4-Va, but not with those prepared from cells transfected with pEGFP-ACTN4-Ub or the parental pEGFP-C1 vector (ACTN4-Va, Figure 1B). On the other hand, the monoclonal antibody 13G9 reacted with both the ubiquitous and variant actinin-4 proteins (pan-ACTN4, Figure 1B).

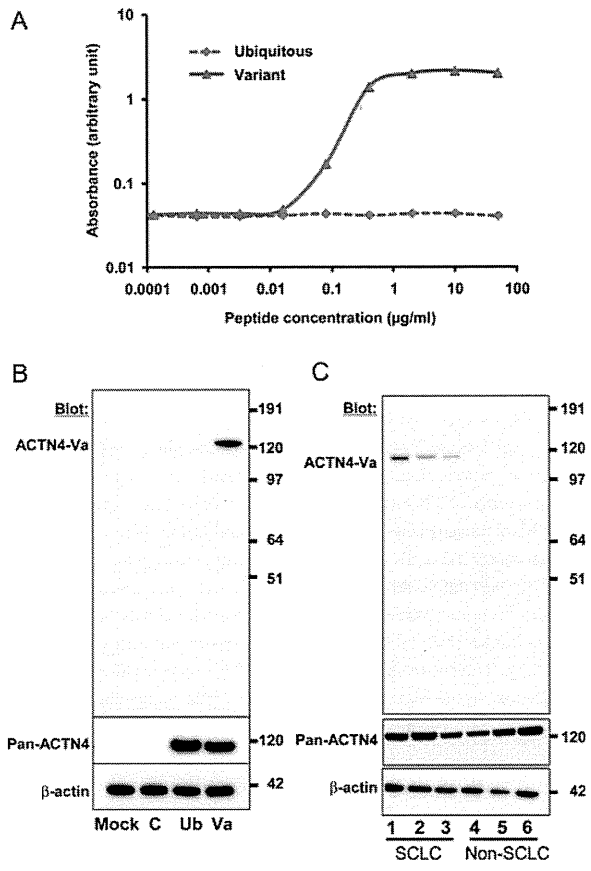

Figure 1. Specificity of the 15H2 monoclonal antibody to the actinin-4 variant. (A) Reactivity of the 15H2 monoclonal antibody with the synthetic peptides DIVNTARPDEKAIMTYVSS (ubiquitous) and DIVGTLRPDEKAIMTYVSC (variant), as determined by the antibody capture assay. (B) Proteins were extracted from HEK293 cells that had been transfected with no plasmid (mock), pEGFP (C), pEGFP-ACTN4-Ub (Ub) or pEGFP-ACTN4-Va (Va) and blotted with 15H2 (ACTN4-Va), 13G9 (pan-ACTN4) and anti-β-actin (loading control) antibodies. Molecular masses (in kiloDaltons) are shown on the right. (C) Proteins were extracted from three small cell lung carcinoma (SCLC) cell lines [SBC3- (lane 1), Lu-135 (2) and Lu-165 (3)] and three non-small cell lung carcinoma (NSCLC) cell lines [LCD (4), LK-2 (5) and EBC-1 (6)] and blotted with 15H2 (ACTN4-Va), 13G9 (pan-ACTN4) and anti-β-actin (loading control) antibodies. Molecular masses (in kiloDaltons) are shown on the right.

The expression of endogenous variant actinin-4 was detected in all three SCLC cell lines examined (SBC-3, Lu-135 and Lu-165), but in none of the three non-SCLC cell lines (LCD, LK-2 and EBC-1) (Figure 1C), being consistent with the results of cDNA sequencing described above.

significance of variant actinin-4 expression in the diagnosis of HGNT

We next investigated immunohistochemically the expression of both actinin-4 proteins and classical NE markers (CGA, SYN and CD56) in 609 primary lung tumours. Representative results of immunohistochemical staining are shown in Figure 2, and the positivity rates for each histological subtype are summarized in Table 1. CGA was expressed in 88% (59/67) of SCLCs and 56% (59/105) of LCNECs. SYN was expressed in 88% (58/66) of SCLCs and 56% (59/105) of LCNECs. CD56 was expressed in 96% (64/67) of SCLCs and 72% (76/105) of LCNECs. The three NE markers were also expressed in 76%–100% of pulmonary carcinoid tumours (Table 1). The expression of variant actinin-4 protein was detected in 55% (96/176) of HGNTs [60% (42/70) of SCLCs and 51% (54/106) of LCNECs], but in only 10% (5/51) of carcinoid tumours. The difference in the frequency of variant actinin-4 expression between HGNTs and carcinoid tumours was statistically significant ($P = 6.0 \times 10^{-6}$, Fisher's exact test).

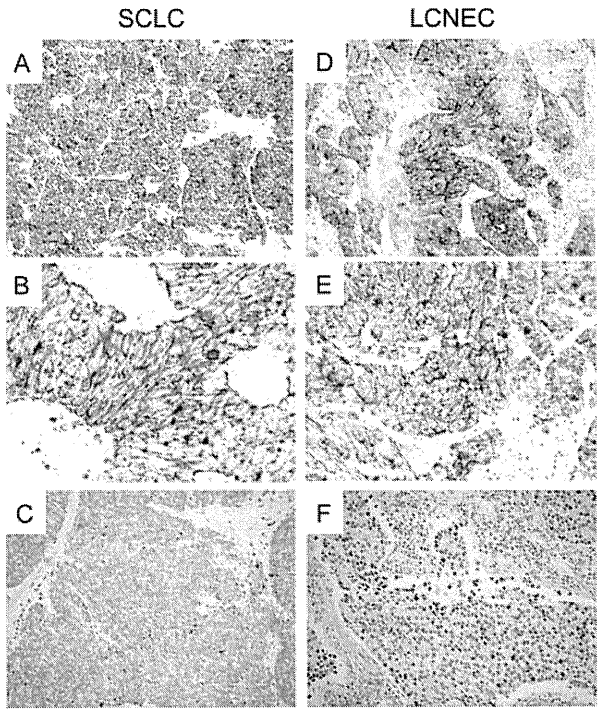

Figure 2. Expression of the variant actinin-4 protein in high-grade neuroendocrine tumour (HGNT). Representative cases of small cell lung carcinoma (SCLC) (A–C) and large cell neuroendocrine carcinoma (LCNEC) (D–F) showing positive (A, B, D and E) and negative (C and F) immunoreactivity with the 15H2 monoclonal antibody. Original magnification: A, C, D and F, ×20; B and E, ×400.

CGA, SYN and CD56 were found to show variable expression in non-NE lung tumours (2%–11% of adenocarcinomas, 2%–14% of squamous cell carcinomas and 6%–17% of other NSCLCs). However, variant actinin-4 protein was expressed in only 0.8% (3/382) of non-NE NSCLCs. These results indicated that variant actinin-4 was highly specific to HGNTs.

prognostic significance of variant actinin-4 expression

There was no significant difference between patients with HGNTs that were positive ($n = 96$) and negative ($n = 80$) for variant actinin-4 protein expression with respect to gender, age, smoking status, histological subtype (LCNEC versus SCLC), pathological stage, tumour size or frequency of lymph node or distant metastasis (Table 2). However, the frequency of relapse after surgery was much higher in stage I to III HGNT cases that were positive for variant actinin-4 protein expression [67% (53/79)] than in cases that were negative [43% (39/91)] ($P = 0.0020$, Fisher's exact test) (Table 2). The sites of first recurrence in patients with HGNTs that were positive for variant actinin-4 expression included the brain (16 cases), lymph nodes (16 cases), lung (9 cases), liver (6 cases), and bone (5 cases), but the site distribution did not differ significantly from that in negative cases.

The overall survival of patients with variant actinin-4-positive HGNT, SCLC and LCNEC was significantly worse than that of patients whose tumours were negative [$P = 0.00021$ (HGNT, Figure 3A), 0.0283 (SCLC, supplementary Figure S3A, available at *Annals of Oncology* online) and 0.0022 (LCNEC, supplementary Figure S3B, available at *Annals of Oncology* online), log-rank test]. Furthermore, progression-free survival also differed significantly between patients whose tumours were positive and negative for variant actinin-4 expression [$P = 0.0021$ (HGNT, Figure 3B), 0.018 (SCLC, supplementary Figure S3C, available at *Annals of Oncology* online) and 0.048 (LCNEC, supplementary Figure S3D, available at *Annals of Oncology* online), log-rank test]. The 5-year survival rates of patients with variant actinin-4-negative HGNT, SCLC and LCNEC were 62%, 62% and 62%, respectively, whereas those of

Table 1. Expression of variant actinin-4 and three NE markers in various histological subtypes of lung cancer

Histological subtype[a]	*N*	Variant actinin-4	CGA	SYN	CD56
SCLC	70	42 (60%)	59 (88%)	58 (88%)	64 (96%)
LCNEC	106	54 (51%)	59 (56%)	59 (56%)	76 (72%)
Carcinoid	51	5 (10%)	49 (100%)	49 (100%)	37 (76%)
Adenocarcinoma	164	1 (1%)	16 (11%)	6 (4%)	4 (2%)
Squamous cell carcinoma	166	2 (1%)	23 (14%)	4 (2%)	16 (10%)
Others	52	0 (0%)	9 (17%)	5 (10%)	3 (6%)

SCLC, small cell lung carcinoma; LCNEC, large cell neuroendocrine carcinoma; NE, neuroendocrine; CGA, chromogranin A; SYN, synaptophysin; IARC, International Agency for Research on Cancer; WHO, World Health Organization.

[a]Based on the Pathology and Genetics of Tumours of the Lung, Thymus and Heart (IARC WHO Classification of tumours) (third version, 2004).